

Cite this: DOI: 10.1039/c0xx00000x

www.rsc.org/xxxxxx

ARTICLE TYPE

Mechanistic pathways in aromatic nucleophilic substitution in conventional solvents and ionic liquids.

Marcela Gazitúa,^{a*} Ricardo A. Tapia,^b Renato Contreras^c and Paola R. Campodónico^a

Received (in XXX, XXX) Xth XXXXXXXXXX 20XX, Accepted Xth XXXXXXXXXX 20XX

DOI: 10.1039/b000000x

Solvation effects on the reaction mechanism of the title reactions have been kinetically evaluated for 21 conventional solvents and 17 ionic liquids. Solvent polarity affects the catalyzed and non catalyzed S_NAr pathways differently. The amphiphilic character of water and formamide which act as hydrogen bond donor/acceptor induces nucleophilic activation at the nitrogen center of the nucleophile. The ionic liquid EMIMDCN appears as the best solvent for the S_NAr route probably due to the high polarizability of dicyanamide anion.

Introduction

Nucleophilic substitution is an addition/elimination process that depending on the nature of the substrate, the attacking nucleophile and the solvent effect may lead a nucleophilic substitution (S_N) product, a nucleophilic aromatic substitution (S_NAr) product, or both.¹ Scheme 1 summarizes the possible routes towards any of both reaction products. When the reaction center is a heteroatom (left branch in Scheme 1) the reaction mechanism is S_N and it depends on the stability of the pentavalent intermediate (P[±] in Scheme 1) formed. If P[±] is not stabilized under the reaction conditions, the process is concerted.² Conversely, if P[±] is stabilized, a stepwise pathway may be operative.¹ Furthermore, if the nucleophilic attack occurs at the aromatic ring (right branch in Scheme 1), the reaction is classified as S_NAr.^{1,3-8} This reaction proceeds via stepwise mechanism^{1,3-6} that involves: i) a nucleophilic attack with re-hybridization at the ipso carbon atom on the aromatic ring from sp² to sp³ to form a Meisenheimer Complex^{1,7,8} (MC1 in Scheme 1) and ii) the leaving group (LG) departure in a second step to regenerate the sp² center through catalyzed or non catalyzed pathways^{1,4-8} (k₃ or k₂, respectively in Scheme 1).

Solvent effects on S_NAr reactions have previously been studied for conventional organic solvents (COS)^{4,8-11} and more recently in room temperature ionic liquids (RTILs).¹²⁻¹⁶ The main focus in these studies was put on the bulk and specific solute-solvent interactions that determine selectivity, reaction rates and mechanisms in these systems. Nudelman et al.⁹ studied leaving group abilities in the S_NAr reactions of halobenzenes towards amines in aprotic COS. These authors found that the rate-limiting step of the reaction mechanism changes when the reaction proceeds in solvents that exhibit hydrogen-bond basicity (HBB) properties. Wang et al.¹⁰ reported that HBB of solvents significantly affect the regiochemistry of the S_NAr reaction between polyfluoroarene derivatives with amines. Park et al.¹¹

investigated the mechanism of S_NAr of fluorination reactions under the influence of protic solvents and charged nucleophiles. They found that counterion or protic solvent alone retards the S_NAr reactions, while together they promote enhancement of reactivity. For these systems, the protic solvent may affect the reaction acting over the counterion as a Lewis base, and the nucleophile acting as an ion pair. The presence of charges, as separated cation/anion pair or as ion pairs strongly suggest that these results may be used to study solvent effects on chemical reactivity (reaction rates in the present case) in RTILs. D'Anna et al.¹⁴ recently reported on the reaction of thiophene derivatives with N-nucleophiles in RTILs. They propose that the intramolecular interactions at the transition state structure are strongly affected by the reaction medium, determining the selectivity and catalysis of the process.

These backgrounds prompted us to perform a comparative study of solvation effects in COS and a series of RTILs. However, some preliminary considerations are worth stressing. First of all, the physical interpretation of solvent effects in RTILs is an extremely complex problem, because in general, good RTILs (as reaction media) are those species where the anion and cation are associated to a very low extent.¹⁷ This result implies that the target solute-solvent interactions will in general be masked by the leading solvent-solvent interactions that are coulombic in nature. A usual experimental model to rationalize solvation effects on reaction rates in RTILs media is to take a reasonable large number of RTILs (17 in the present case) and evaluate their performance as reaction media by fixing the anion and varying the cation and vice versa. The criteria for selecting the series of RTILs were based on: (i) the solubility of substrates and nucleophiles; (ii) to have a reasonable number of anions and cations to assess anion and cation effects and to ensure that these RTILs do not interfere with the reaction under study. Scheme 2 shows structures and acronyms of the RTILs used in this study.

5



10

BMIM	EMIM	BMPL	HMIM	BM₂IM	MOEDEA
Anions:					
FAP	DCN	PF₆	NTf₂	SCN	
RTIL:					
EAN					

Results and discussion

In this work we use the reaction of 2,4-dinitrophenylsulfonyl chloride (**DNBSCI**) towards secondary alicyclic (SA) amines in aqueous media as a model system to analyze the effect of solvent polarity on the reaction mechanism. We started with the synthesis of 1-(2,4-dinitrophenylsulfonyl)piperidine and 1-(2,4-dinitrophenyl)piperazine (compounds **2** and **3** in Scheme 1), corresponding to the S_N and S_{NAr} reaction products, respectively (Synthetic details are given in Experimental Section). The product analysis in water and in acetonitrile (MeCN) shows that **3** is the unique product at the end of the reaction, thereby suggesting a S_{NAr} pathway. HPLC analyses were performed to compare the retention times and UV-visible spectra with those of authentic samples in water and in MeCN as reaction media at the end of the reaction. (See Figures S1-S9 in Electronic Supplementary Information (ESI)). However HPLC analyses at different times show that the S_N product is formed in minor proportion and decomposed in excess of amine to give the S_{NAr} product in both cases (see Figures S8 and S9 in ESI).

The formation of a unique S_{NAr} product discards the possibility of nucleophilic attack at the unsubstituted position on the ring.¹⁸ Under amine excess, pseudo first order rate constant (k_{obs}) were found for all the reactions. The values of k_{obs} for all the reactions are in accordance with Eqn. 1 were k_0 and k_N are the rate coefficients for solvolysis and aminolysis of the substrate, respectively. These values were obtained as the intercept (k_0) and slope (k_N) of linear plots of Eqn. 1 for the reactions of **DNBSCI** with all amines in water, some COS and all RTILs.

$$k_{obs} = k_0 + k_N[N] \quad \text{Eqn 1.}$$

In water, for all amines studied, linear plots of k_{obs} vs. free amine concentration ($[N_F]$) is observed. These plots pass through the origin, thereby suggesting that the contribution of hydroxide and/or water (i.e., the k_0 step in Scheme 1) to the pseudo first order rate constant (k_{obs}) values is negligible⁸ and the reactions occurs via a non catalyzed route (k_2 in Scheme 1). Kinetic details are shown in Experimental Section and ESI (Figures S10-S15 and Tables S1-S15).

Previous reports suggest that this kind of reactions proceed through a rate-limiting formation of MC1.^{8,19} However, the statistically corrected Brønsted-type plot for the reference solvent (water) is linear with $\beta_{nuc}=0.8$ a value close to that observed in the ester aminolysis, where the LG departure is rate determining.²⁰ It seems then that the bond formation between the nucleophiles and the substrate is fully advanced in the rate-limiting transition state. Table 1 shows the nucleophilic rate constants and pK_a values in water needed to build up the Brønsted type-plot. Note that, piperidine is a basic amine that tends to deprotonate more easily which is in agreement with k_N values found for SA amines.

Table 1. pK_a and k_N values for the reactions of SA amines with **DNBSCI** in water.

Amine	pK_a^{21}	$10^4 k_N / s^{-1}M^{-1}$
Piperidine	11.24	306.4 ± 4.8
Piperazine	9.94	51.9 ± 0.78
1-(2-Hydroxyethyl)piperazine	9.39	16.1 ± 0.22
Morpholine	8.78	4.95 ± 0.14
1-Formylpiperazine	7.68	0.786 ± 0.04

^a The value accompanying the k_N values correspond to error of the slope of a plot of k_{obs} vs free amine concentration required to build up Brønsted plots.

In order to examine the solvent effects on the reaction mechanism, we studied the reaction between **DNBSCI** and piperidine in a series of 20 COS and 17 RTILs using the reaction in water as reference. For all reaction media, the final product was confirmed to be compound **3**, thereby ratifying a S_{NAr} pathway.

Linear plots of k_{obs} vs. $[N_T]$ (total amine concentration) for a series of COS and the whole series of RTILs series are coincident with the same kinetic responses found in aqueous media (see Figures S16-S41 and Tables S16-S42 in ESI). However, some COS shows curvature upward as a function of increasing amine concentration. Such curvature is typical for reactions that proceed through a rate limiting proton transfer (RLPT) mechanism²² (MC2, right side branch in Scheme 1). Details are given in Figures S42-S67 and Tables S43-S55 in ESI. According to Scheme 1, the reaction proceeds through two intermediates (MC1 and MC2) corresponding to a zwitterionic adduct and its deprotonated form, respectively. Table 2 shows the microconstants Kk_2 and Kk_3 for the reaction of **DNBSCI** with piperidine for a series of COS studied that proceeds through catalyzed pathways. The low contribution of Kk_2 (to promote the LG departure) and Kk_3 (to promote the stabilization of MC2) show that solvents effects are small in these cases. This result may be traced to the presence of a second molecule of amine that could establish a more favoring interaction to the MC1 compared to that of the solvent molecules. However, solvent polarity may become relevant in the non catalyzed route.

Table 2. Observed microconstants Kk_2 and Kk_3 for the reaction of DNBSCl with piperidine in a series of catalyzed processes in COS.^a

Solvent	$10^3 Kk_2 / s^{-1}M^{-1}$	$10^1 Kk_3 / s^{-1}$
MeCN	7.25 ± 0.347	0.780 ± 0.0223
THF	0.372 ± 0.0600	0.211 ± 0.00350
CH_2Cl_2	1.31 ± 0.317	0.640 ± 0.0204
$CHCl_3$	0.500 ± 0.116	0.120 ± 0.00620
C_6H_6	1.86 ± 0.314	0.500 ± 0.0170
DMF	8.75 ± 0.191	0.270 ± 0.0106
1,4-Dioxane	0.403 ± 0.109	0.163 ± 0.00820
Acetone	1.53 ± 0.254	0.452 ± 0.0190
Cyclohexane	1.94 ± 0.295	0.85 ± 0.0356
Diethyl Ether	1.76 ± 0.420	0.320 ± 0.0320
Ethyl Acetate	1.14 ± 0.210	0.300 ± 0.0136
n-Hexane	0.0454 ± 0.431	0.791 ± 0.0402
n-Heptane	0.0328 ± 0.452	1.04 ± 0.0563

^a The value accompanying to the Kk_2 and Kk_3 values correspond to the error of the slope (for Kk_2) and the intercept (for Kk_3).

The “polarity of the solvent” is a rather ambiguous concept, because it encompasses a series of different effects, namely, the static polarizability (dielectric effects) of the solvent; (electronic) polarization of the solvent and specific solute-solvent interactions (typically, hydrogen bonding effects). Kamlet-Taft's linear solvation energy relationship (LSER)²³⁻²⁶ model does the job in the sense that solvent effects on rate constants may be described by the Hydrogen Bond Acidity (HBA) parameter α ; the HBB parameter β and the π^* parameter²¹ (see Table 3).

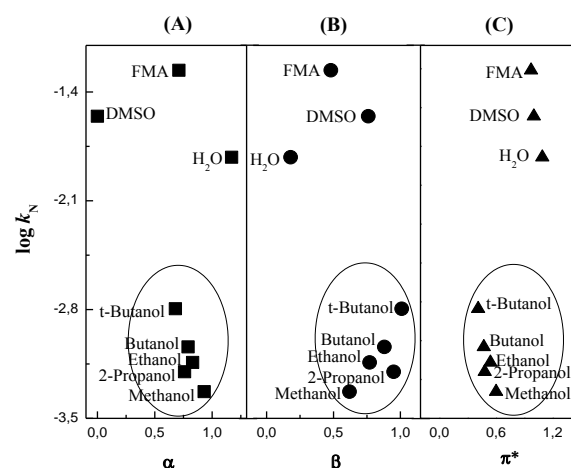
Table 3. Values of k_N for the reactions of DNBSCl with piperidine in a series of non catalyzed processes in COS and their Kamlet-Taft parameters.

Solvent	$10^4 k_N / s^{-1}M^{-1}$	α^{23}	β^{23}	π^{*23}
DMSO	278 ± 9	0.0	0.76	1.0
Ethanol	7.2 ± 0.30	0.86	0.84	0.48
FMA	547 ± 11	0.71	0.48	0.97
H ₂ O	156 ± 2.2	1.17	0.18	1.09
tert-Butanol	16.4 ± 0.90	0.68	0.93	0.41
2-Propanol	6.4 ± 0.29	0.76	0.84	0.48
Butanol	9.2 ± 0.43	0.84	0.84	0.47
Methanol	4.8 ± 0.12	0.98	0.66	0.60

k_N values were obtained from the slope of a plot of k_{obs} vs. total amine concentration.

Figure 1(A) shows the relationships between $\log k_N$ for the non catalyzed reactions and α parameter²³ which is associated with HBA ability of solvents. In figure 1(A) we have two regions

independently of their α values. In the first one, we found dimethylsulfoxide (DMSO), formamide (FMA) and H₂O grouped as being the best solvents in terms of rate coefficients. On the other hand, we found a second group including all alcohols used in this study. Here there are two points worth mentioning: one is that DMSO, H₂O and FMA are more polar than alcohols and secondly that they display different hydrogen-bond (HB) accepting/donating abilities. For instance, DMSO presents only HB accepting properties, while H₂O and FMA can accept and donate HB. The high rate value for H₂O suggests the presence of a HB between a hydrogen atom of H₂O acting as a bridge between the nucleophile and the leaving group at the MC1 structure. This bridge facilitates the relay of electron density from the amine towards the electrophilic centre; thereby enhancing the nucleophilicity of the amine (see Figure 2).⁵

**Figure 1.** Plots of $\log k_N$ and α (A), β (B) and π^* (C) for the reactions of DNBSCl with piperidine in a series of non catalyzed processes in COS.

We further performed the kinetic analysis of the reaction in 50% w/w ethanol/water mixture and 90% w/w ethanol/water mixture under the same experimental conditions (see Table S43 in ESI), in order to compare the role of HB effects in these mixtures with water. The rate coefficient H₂O vs. 50/50 ethanol/water mixture ratios are 5 times slower while that of H₂O vs. 90/10 ethanol/water mixture are 9 times slower. This result suggests that there may be an increase in reactivity induced by “preferential solvation” in favor of the aqueous phase.⁴ Probably; FMA can also form effective HB to the nucleophile and the leaving group at the MC1 structure. These properties of FMA and H₂O should account for the high k_N values observed.

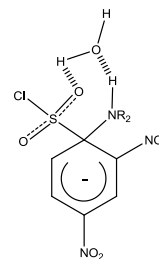


Figure 2. General scheme for the possible interaction between H₂O and MC1 intermediate.

Note that all alcohols have high values of α parameters, but low k_N values. This can be traced to its low polarity compared to that of DMSO, FMA and H₂O.

Figure 1(B) shows the relationship between $\log k_N$ and β parameter,²³ which is a measure of HBB ability of solvents. Figure 1(B) displays the same separations between solvents of varying polarity. Here again we have two regions independently of their β values that are worth analyzing. In the first one we found solvents with HB accepting (DMSO) and HB accepting/donating (FMA and H₂O) abilities that can interact with the proton of piperidine, thereby increasing the electron density on the nitrogen atom.²⁵ Note that alcohols appear grouped with the same pattern as that shown in Figure 1(A).

Figure 1(C) shows the relationships between $\log k_N$ and π^* parameter,²³ which measures the ability of solvents to stabilize a neighboring charge or a dipole by virtue of nonspecific dielectric interactions. Note that the trend is similar to that found for α and β values shown in Figures 1A and 1B. In this Figure we have two regions differing in solvent polarity and independently of their π^* values. Since H₂O, FMA and DMSO have the highest π^* values among all the solvents investigated these reaction media enhance the reaction.

Table 4 shows k_N values for the reactions of DNBSCI with piperidine in RTILs and their Kamlet-Taft parameters.

Table 4. Values of k_N for the reactions of DNBSCI with piperidine in RTILs and their Kamlet-Taft parameters.

RTILs	$10^4 k_N / s^{-1} M^{-1}$	α	β	π^*
EAN	8.70 ± 0.35	0.85^{27}	0.46^{27}	1.24^{27}
BMIMPF ₆	207 ± 10.0	0.65^{28}	0.25^{28}	1.02^{28}
EMIMSCN	480 ± 50.0	nd	nd	nd
BMIMBF ₄	448 ± 42.0	0.63^{28}	0.39^{28}	1.04^{28}
EMIMBF ₄	489 ± 28.0	nd	nd	nd
MOEDEAFAP	152 ± 6.30	nd	nd	nd
EMIMFAP	179 ± 17.0	nd	nd	nd
BMIMFAP	186 ± 5.60	nd	nd	nd
BMPLFAP	194 ± 10.0	nd	nd	nd
BMIMDCN	235 ± 5.30	0.54^{28}	0.60^{28}	1.05^{28}
BMPLDCN	299 ± 17.0	nd	nd	nd
EMIMDCN	717 ± 32.0	0.54^{27}	0.64^{27}	1.07^{27}
BMIMNTF ₂	266 ± 21.3	0.72^{28}	0.24^{28}	0.90^{28}
EMIMNTF ₂	360 ± 19.0	0.71^{28}	0.23^{28}	0.98^{28}
BMPLNTF ₂	330 ± 28.0	0.57^{28}	0.23^{28}	0.87^{28}
BM ₂ IMNTF ₂	263 ± 15.0	0.38^{28}	0.26^{28}	1.02^{28}
HMIMNTF ₂	291 ± 20.0	0.65^{28}	0.26^{28}	0.97^{28}

nd: no data available in literature. k_N values was obtained from the slope of a plot of k_{obs} vs total amine concentration.

Figure 3 displays linear relationships between k_{obs} and $[N_T]$ for the same reaction in the series of 17 RTILs. The comparisons will be made taking water as reference. We can identify the following classification of the ionic solvents: i) best solvent: EMIMDCN, ii) good solvents: BMIMBF₄, EMIMSCN, EMIMBF₄, BMIMNTF₂, BM₂IMNTF₂, HMIMNTF₂, BMPLNTF₂, EMIMNTF₂, BMIMFAP, BMPLFAP, BMIMPF₆, BMIMDCN and BMPLDCN, iii) similar to water: MOEDEAFAP and EMIMFAP and iv) very poor solvent: EAN.

EAN is the only protic solvent that decreases the reaction rate 17 times vs. H₂O and 82 times vs EMIMDCN. EMIMDCN behaves as the best solvent within the series of 38 reaction media analyzed in this work, that presents catalytic behavior at room temperature and therefore it qualifies as the best solvent for this S_NAr reaction. Note that EMIMDCN exert its catalytic property for the pathway that does not involve a second nucleophilic molecule as catalyst. The pK_a value of dicyanamide is less than 1.²⁹ As a result, the nucleophilicity on the nitrogen of piperidine is enhanced. The MC1 forming step is expected to be fast and the leaving group departure becomes rate determining.

If we compare the k_N values of Table 3 for COS and Table 4 for RTILs we can see that for this S_NAr reactions RTILs performs relatively well in comparison with COS.

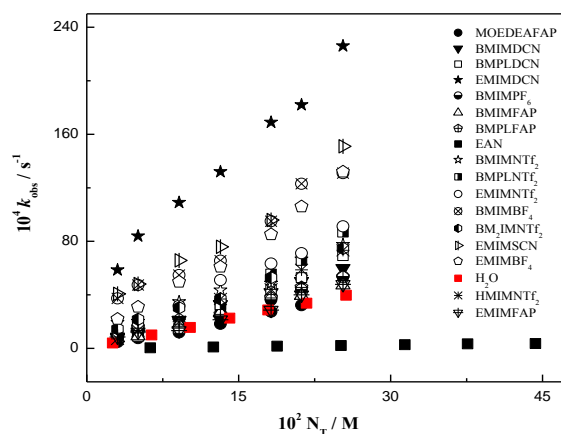


Figure 3. Plot of k_{obs} against total amine concentration $[N]_T$ of piperidine for the reactions of DNBSCI with piperidine in a series of RTILs taken H₂O as reference (red squares).

If we make the analysis of solvent polarity using Kamlet-Taft's linear solvation energy relationship (LSER)²³⁻²⁶ the comparison of COS vs. RTILs present the problem that for the latter, a charged probe should be used, to account for the cation-anion interaction and the performance depends on the solvatochromic dyes used.²⁵ The large variations found in LSER values given by different dyes used, prevent a direct comparisons of results obtained with different probe in the same analysis.²⁵

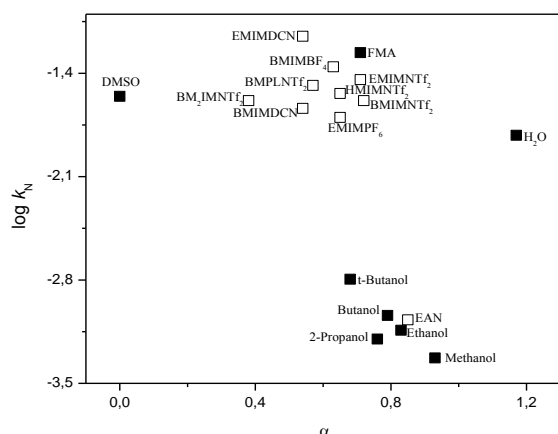


Figure 4. Plots of $\log k_N$ for the reactions of DNBSCI with piperidine in a series of COS and RTILs against α .

Figure 5. Plots of $\log k_N$ for the reactions of DNBSCI with piperidine in a series of COS and RTILs against β .

Figure 5 shows the relationships between $\log k_N$ and β parameter²³ for COS shown in Figure 1 and RTILs. β value of an RTIL is controlled primarily by the anion, with basicity increasing as the strength of the conjugate acid of the anion decreases; and its antagonistic possibility of HBA on the cation.²⁵ Figure 5 display similar trends to those shown in Figure 4. Here again we have two regions grouped independently of their β value.

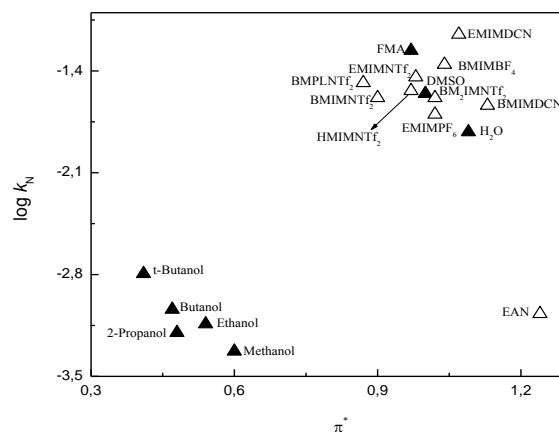
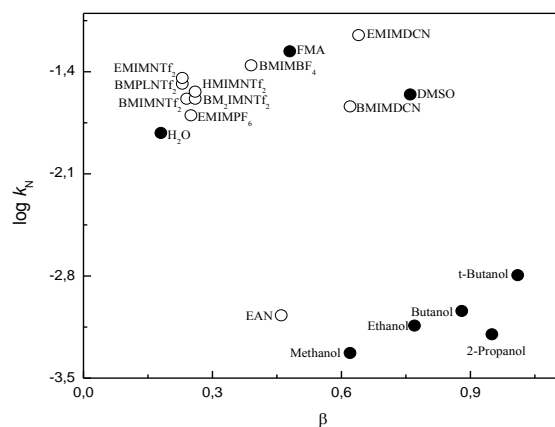


Figure 6. Plots of $\log k_N$ for the reactions of DNBSCI with piperidine in a series of COS and RTILs against π^* .

Figure 6 shows the relationship between $\log k_N$ and π^* parameter²³ for COS shown in Figure 1 and RTILs.

Welton et al.³⁰ found that all the RTILs they used presenting high values of π^* , with little variation between them, should always lead to an increased rate for its and similar reactions. Apparently, in our case, this applies for all RTILs studied except for EAN that present a high π^* value and a low rate constant. Note that here again the polarity of the medium is determinant in the stabilization of the intermediate and therefore on the reaction rate. To close our study, we made an additional analysis performed by fixing the cation (EMIM in the present case) and varying the anionic counterpart (i.e. to evaluate anion effect). Figure 7 and 8 summarize the comparison between k_{obs} and $[N_T]$ for the EMIM and NTf₂ series, respectively. Other comparisons are shown in ESI (Figures S68-S71).

Following a suggestion made by a reviewer, we performed a complete multiparametric correlation among our $\log k_N$ and the Hydrogen bond acidity (α), the Hydrogen bond basicity (β) and solvent polarity (π) Kamlet-Taft (KT) solvent parameters taken from literature. The KT analysis of solvation effects shows similar trends to that shown in Figures 4-6 obtained from a one parameter plot. These correlations are reported in ESI, Figures S72-S73.



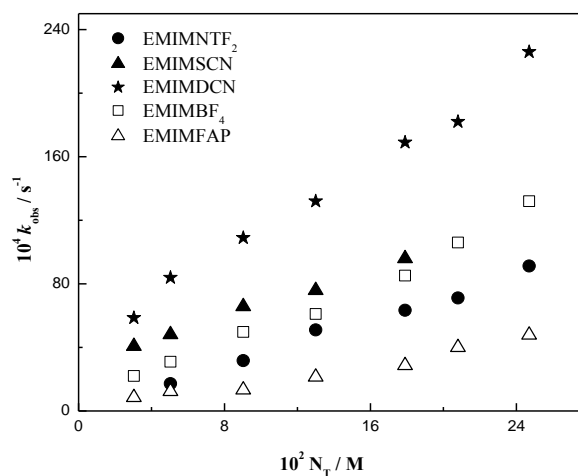


Figure 7. Comparison between k_{obs} against total amine concentration $[N_T]$ for the reaction of DNBSCl with piperidine in EMIMNTF₂, EMIMSCN, EMIMDCN, EMIMBF₄ and EMIMFAP at 25.0 °C.

The results show the following order of decreasing quality as reaction media: [DCN]⁻ > [SCN]⁻ > [BF₄]⁻ > [NTF₂]⁻ > [FAP]⁻. This result may be attributed to the significantly high polarizability of dicyanamide anion, which presents a highly rich π electron density. An additional factor seems to be the size of the anion which shows an inverse relationship with reaction rate. Even though we do not have enough information to rationalize these results it could be related to steric hindrance effects.

We considered a similar analysis but this time fixing the anion [NTF₂]⁻ and varying the cation. No significant differences in reaction rates were observed by changing the length of the alkyl chain of the imidazole from two to six carbons, even if the acidic proton of the imidazole is blocked. (See Figure 8). Apparently, the steric hindrance effects going from two to six carbon atoms in the alkyl chain in the cation is less important than changes in the size of the anion.

An striking observation is that EMIMDCN and BMIMDCN only differing in alkyl chain on the cation display quite different rate coefficients. One possibility is to have both RTILs with significant amount of water. We proceeded then to repeat the kinetic measurements after drying both solvent for 8 hours into a vacuum drying oven at a pressure of -0.06 MPa. The same kinetic results were obtained. It seems that kinetic data are not sufficient to settle this differences which could be elucidated with the aid of theoretical studies introducing electronic structures informations. Work along this line is in course in our group.

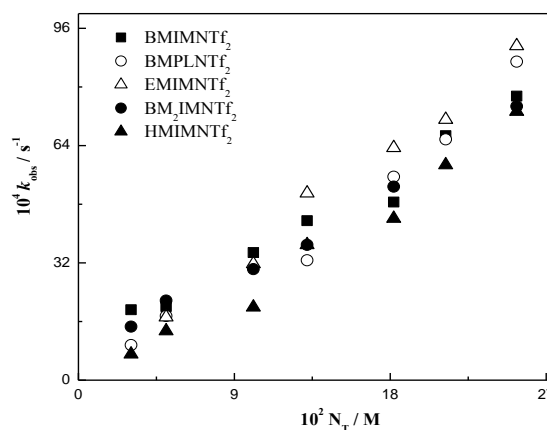


Figure 8. Comparison between k_{obs} against total amine concentration $[N_T]$ for the reaction of DNBSCl with piperidine in BMIMNTF₂, EMIMNTF₂, BMPLNTF₂, EMIMNTF₂, BM₂IMNTF₂ and HMIMNTF₂ at 25.0 °C.

Conclusions

Solvation effects on the reaction mechanism of the title reactions have been kinetically evaluated for a set of 21 conventional solvents and 17 RTILs. Solvent polarity affects the catalyzed and non catalyzed S_NAr pathways differently. Competitive S_N product is not observed at the end of the reaction under pseudo first order conditions verified by HPLC analyses. The study of solvent polarity performed on the series of COS plus water and FMA reveals that HB ability drives the S_NAr process in the non catalyzed route in Scheme 1. The role of water and FMA is the most significant due to its amphiphilic character as HB donor and HB acceptor that result in a nucleophilic activation at the nitrogen center of piperidine. It is relevant to note that RTILs performed relatively well in comparison with COS. The ionic liquid EMIMDCN appears as the best solvent for this S_NAr route, a result probably due to the high polarizability of dicyanamide anion.

Experimental section

Materials

Piperidine was purified before used. All the solvent used were commercial available by Sigma-Aldrich and Merck with purity \geq 99%, stored under anhydrous conditions and used as received. The certificate of analysis given by Merck S.A. of all RTILs show purity values between 99 and 100%, presence of halides \leq 0.1 % and his content of water \leq 1 %. To ensure that they had no water, we put the RTILs into a vacuum drying oven LabTech Model LVO-2013 for 4 hours at a pressure of -0.06 MPa before used.

Synthetic protocol of 1-(2,4-dinitrophenyl)piperidine.

To a solution of 1-chloro-2,4-dinitrobenzene (200 mg, 0.99 mmol) in dry DMSO (2.0 mL), containing potassium carbonate

(280 mg, 2.03 mmol), was added piperidine (169 mg, 1.98 mmol). The mixture was stirred for 12 h at room temperature and the reaction mixture was poured onto ice-water (20 g). The solid was filtered, washed with water, dried and recrystallized from ethanol to give 1-(2,4-dinitrophenyl)piperidine (180 mg, 73%), mp 92–93 °C (Lit.³¹ 91–92.5 °C). ¹H (400 MHz, CDCl₃): δ 1.65–1.80 (m, 6H), 3.20–3.30 (m, 4H), 7.08 (d, J = 9.4 Hz, 1H), 8.21 (dd, J = 9.4, 2.7 Hz, 1H), 8.69 (d, J = 2.7 Hz, 1H).

10 Synthetic protocol of 1-(2,4-dinitrophenylsulfonyl)piperidine.

To a solution of 2,4-dinitrobenzenesulfonyl chloride (2.67 g, 10 mmol) in dichloromethane (35 mL), was added with slow drip piperidine (0.85 g, 10 mmol) at 0 °C. The mixture was stirred for 4 hours and the reaction mixture was diluted with dichloromethane (50 mL), washed with 1N HCl (15 mL), brine and dried. The solvent was removed under reduced pressure and the residue was purified by column chromatography on silica gel using ethyl acetate-hexane 1:5 to give 1.85 g of a white product (59%), mp 128–130 °C (Lit.³² 130 °C). ¹H NMR δ 1.58–1.80 (m, 2H), 1.80–1.84 (m, 4H), 3.54–3.70 (m, 4H), 8.21 (d, J = 8.6 Hz, 1H), 8.45 (d, J = 2.0 Hz, 1H), 8.49 (dd, J = 2.0, 8.6 Hz, 1H).

Kinetic Measurements.

The kinetics of the reactions were measured by a diode array spectrophotometer in water at 25.0 °C and an ionic strength of 0.2 M (maintained with KCl), by monitoring (380 nm) the formation of product **3**. The kinetic measurements in COS, RTILs and 90/10 ethanol/water mixture were in absence of KCl and at 350–400 nm at the same temperature. The initial substrate concentration was 5 × 10⁻⁵ M. Under excess amine, pseudo-first-order rate coefficients (*k*_{obs}) were found throughout. For the reactions via non catalyzed the *k*_{obs} values were obtained through the kinetic software (for first-order reactions) of the spectrophotometer. For the reactions via catalyzed, the validation that the reaction proceeds as shown Scheme 1 is through of plots of *k*_{obs}/[N_T] vs. [N_T] are linear. *Kk*₂ values are obtained from the intercept of these graphs and *Kk*₃ is obtained from the slope of these graphs.

40 Chromatographic system and conditions.

The HPLC system used for the analysis of the samples was a UV-DAD Elite Lachrom with quaternary pump L-2100 with a UV-DAD detector L-2455, 8 μL injection loop, oven column L-2300 and autosampler L-2200 with cooling unit. The column attached was a Chromolith Fast Gradient RP 18 50-3mm (Merck). The UV detector was set at 260 nm which was found to be the most suitable wavelength for the detection of all the substrates, product and internal standard. The flow-rate of the mobile phase was adjusted to 0.5 mL/min to keep the column pressure between 47 – 50 bar. The system was thermostated at 25 °C, to maintain the same reactions conditions. Chromatograms were recorded in a computer system using EZChrom Elite software from Agilent.

Acknowledgment

55 This work was supported by Project ICM- P10-003-F CILIS, granted by Fondo de Innovación para la Competitividad del Ministerio de Economía, Fomento y Turismo, Chile; Fondecyt

grants 1100492 and 1110062. M.G. acknowledges support from Conicyt under the postdoctoral fellowship 3120060.

Notes and references

^aCentro de Química Médica, Facultad de Medicina, Clínica Alemana Universidad del Desarrollo, Código Postal 7710162, Santiago, Chile. Fax: 56 2 2327 9639; Tel: 56 2 23279682. E-mail: migazitu@uc.cl;

⁶⁵ pcampodónico@udd.cl

^bFacultad de Química, Pontificia Universidad Católica de Chile, Código Postal 7820436, Santiago, Chile. Tel: 56 2 23544429. E-mail: rtapia@uc.cl

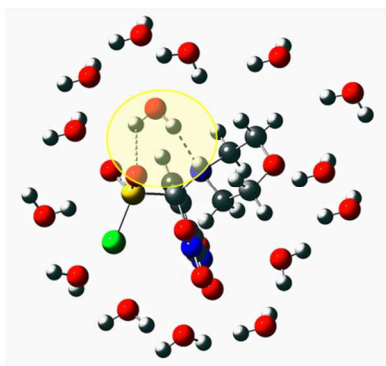
^cDepartamento de Química, Facultad de Ciencias, Universidad de Chile, 70 Casilla 653, Santiago, Chile. Tel: 56 2 29787272. E-mail: rcontrer@uchile.cl

† Electronic Supplementary Information (ESI) available, Copies of ¹H NMR spectra, rate constant values and experimental conditions. This material is available free of charge via the Internet, see DOI: 10.1039/b000000x/

- 1 J. F. Bunnett and R. E. Zahler, *Chem. Rev.*, 1951, **49**, 273; J.-H. Choi, B.-C. Lee, H.-W. Lee and I. Lee, *J. Org. Chem.*, 2002, **67**, 1277; I.-H. Um, J.-Y. Hong, J.-J. Kim, O.-M. Chae and S.-K. Bae, *J. Org. Chem.*, 2003, **68**, 5180; I.-H. Um, S.-M. Chun, O.-M. Chae, M. Fujio and Y. Tsuno, *J. Org. Chem.*, 2004, **69**, 3166; I.-H. Um, J.-Y. Hong and J.-A. Seok, *J. Org. Chem.*, 2005, **70**, 1438.
- 2 A. Williams, *Concerted Organic and Bio-organic Mechanisms*, CRC Press: Boca Raton, FL, 2000, Chapter. 4, pp. 43.
- 3 O. Banjoko and I. A. Babatunde, *Tetrahedron*, 2004, **60**, 4645.
- 4 R. Ormazabal-Toledo, J. G. Santos, P. Ríos, E.A. Castro, P.R. Campodónico and R. Contreras, *J. Phys. Chem. B*, 2013, **117**, 5908.
- 5 R. Ormazabal-Toledo, R. Contreras, R. A. Tapia and P. R. Campodónico, *Org. Biomol. Chem.*, 2013, **11**, 2302.
- 6 R. Ormazabal-Toledo, R. Contreras and P.R. Campodónico, *J. Org. Chem.*, 2013, **78**, 1091.
- 7 C. F. Bernasconi, *MTP Int. Rev. Sci. Org. Chem. Ser. I*, 1973, **3**, 33.
- 8 I.-H. Um, S.-W. Min and J.-M. Dust, *J. Org. Chem.*, 2007, **72**, 8797.
- 9 N. S. Nudelman, P. M. E. Mancini, R. D. Martínez and L. R. Vottero, *J. Chem. Soc. Perkin Trans. 2*, 1987, 951.
- 10 X. L. Wang, E. J. Salaski, D. M. Berger and D. Power, *Org. Lett.*, 2009, **11**, 5662.
- 11 S. Park and S. Lee, *Bull. Korean Chem. Soc.* 2010, **31**, 2571.
- 12 I. Newington, J.M. Perez-Arlandis and T. Welton, *Org. Lett.*, 2007, **9**, 5247.
- 13 F. D'Anna, S. Marullo and R. Noto, *J. Org. Chem.*, 2010, **75**, 767.
- 14 F. D'Anna, V. Frenna, R. Noto, V. Pace and D. Spinelli, *J. Org. Chem.*, 2006, **71**, 5144.
- 15 F. D'Anna, S. Marullo and R. Noto, *J. Org. Chem.*, 2008, **73**, 6224.
- 16 C. C. Weber, A. F. Masters and T. Maschmeyer, *Org. Biomol. Chem.*, 2013, **11**, 2334.
- 17 C. A. Angell, N. Byrne and J.-P. Belieres, *Acc. Chem. Res.* 2007, **40**, 1228.
- 18 E. Buncel, J. M. Dust and F. Terrier, *Chem. Rev.*, 1995, **95**, 2261.
- 19 M. R. Crampton, *Adv. Phys. Org. Chem.*, 1969, **7**, 211.
- 20 W. P. Jencks, *Chem. Rev.*, 1985, **85**, 511; E. A. Castro, *Chem. Rev.*, 1999, **99**, 3505.
- 21 E. A. Castro, M. Aliaga, M. Gazitúa and J. G. Santos, *Tetrahedron*, 2006, **62**, 4863.
- 22 F. G. Bordwell and D. L. Hughes, *J. Am. Chem. Soc.*, 1986, **108**, 5991.
- 23 M. J. Kamlet, J. L. M. Abboud, M. H. Abraham and R. W. Taft, *J. Org. Chem.*, 1983, **48**, 2877.
- 24 A. Cerda-Monje, A. Aizman, R. A. Tapia, C. Chiappe and R. Contreras, *Phys. Chem. Chem. Phys.* 2012, **14**, 10041.
- 25 J.P. Hallett and T. Welton, *Chem. Rev.* 2011, **111**, 3508.
- 26 R. Bini, C. Chiappe, V. L. Mestre, C. S. Pomelli and T. Welton, *Org. Biomol. Chem.*, 2008, **6**, 2522.

- 27 P.G. Jossop, D. A. Jossop, D. Fu and L. Phan, *Green Chem.*, 2012, **14**, 1245.
- 28 M. A. Ab-Rani, A. Brant, L. Crowhurst, A. Dolan, M. Lui, N. H. Hassan, J. P. Hallett, P. A. Hunt, H. Niedermeyer, J. M. Perez-Arlandis, M. Shrems, T. Welton and R. Wilding, *Phys. Chem. Chem. Phys.*, 2011, **13**, 16831.
- 29 A. C. Kenneth, *Chemical Kinetics: The study of reaction rates in solution*, Ed. John Wiley & Sons, New York, USA, 1990, pp. 236.
- 30 L. Crowhurst, L. Lancaster, J-M. Pérez-Arlándiz and T. Welton, *J. Am. Chem. Soc.*, 2004, **126**, 11549.
- 31 J. F. Bunnett and G. T. Davis, *J. Org. Chem.*, 1954, **76**, 3011.
- 32 J. D. Loudon and N. Shulman, *J. Chem. Soc.*, 1938, 1926.

15



Solvation effects on the reaction mechanism for nucleophilic substitution reaction have been kinetically evaluated in conventional solvents and ionic liquids.